JOINT INSTITUTE FOR NUCLEAR RESEARCH
The Laboratory of Radiation Biology

FINAL REPORT ON THE INTEREST PROGRAMME

Comprehensive Validation of Geant4-DNA Physics Lists & Nanodosimetric Modeling of Sub-cellular Structures

Supervisor:
Dr. Batmunkh Munkhbaatar

Student:
Matvei Vologzhin, Russia
Tomsk State University

Participation period:
March 2 – April 19,
Wave 14

Dubna, 2026

Contents

Abstract

Galactic cosmic rays pose severe health risks to astronauts, necessitating accurate nanodosimetric modeling. This study, conducted during the INTEREST Wave 14 internship, evaluates the Geant4-DNA toolkit for simulating ion-induced biological damage. The research encompasses three main objectives. First, macroscopic transport parameters (stopping power, range, detour factor) for light and heavy ions were validated against ICRU90 reference data. Second, microscopic Ionisation Cluster Size Distributions (ICSD) were validated against experimental nanodosimetry data (StarTrack and PTB setups) across multiple Geant4 physics lists, confirming the necessity of DNA Option 6 for high-LET particles. Finally, the validated models were applied to simulate ICSD within high-density water approximations of critical sub-cellular structures (histones, ribosomes, cytoskeleton, NMDA receptors) irradiated by various ions (from protons to ^{20}Ne) at 1 MeV/u. These results provide a robust physical baseline for quantifying complex macromolecular radiation damage.

Introduction

Currently, humanity is actively planning and implementing ambitious space missions, particularly deep-space manned flights to the Moon and Mars. These prolonged missions pose severe health risks to astronauts, ranging from acute radiation sickness to late-term carcinogenesis and neurodegenerative disorders. The primary source of these risks is Galactic Cosmic Radiation (GCR). A critical question in modern radiobiology arises: how exactly does cosmic radiation interact with and affect complex biological systems at the fundamental cellular and sub-cellular levels?

The GCR spectrum consists of approximately 85% protons, 10% alpha particles, and 4–5% heavier ions (such as Carbon, Oxygen, Neon, and Iron), with the remaining 1% composed of electrons and positrons. Despite their relatively low flux, heavy charged particles (HZE ions) are of paramount concern due to their high Linear Energy Transfer (LET) and profound biological destructiveness. The effects of such heavy ions on the central nervous system and brain structures are actively investigated at the Laboratory of Radiation Biology (LRB) at JINR [1,2], including experimental evidence of severe clustered DNA double-strand breaks in neurons [3].

To understand the mechanisms of this damage, one must look at the physics of particle interactions. When heavy ions traverse a biological medium—predominantly composed of water (60–80% of total cell mass)—they generate a dense cloud of secondary radiation, primarily delta-electrons. It is the spatial distribution of these inelastic interactions (ionisations and excitations) created by delta-electrons that defines the particle's "track structure" [4]. This nanometric track structure ultimately dictates the complexity of the induced DNA lesions and the subsequent probability of successful cellular repair [5].

Because biological systems are inherently complex, there is no complete analytical theory that can perfectly predict radiation-induced biological effects from first principles. Therefore, sophisticated Monte Carlo simulation toolkits, such as Geant4, are employed. Specifically, the Geant4-DNA extension is utilized to model particle transport and track structure event-by-event down to the electron-volt scale in liquid water [9].

However, before applying these computational tools to complex biological geometries, the underlying electromagnetic physics models (physics lists) must be rigorously validated. This validation must occur at two levels: the macroscopic scale, confirming basic transport parameters against international reference databases [8], and the microscopic (nanodosimetric) scale, ensuring the accurate modeling of ionisation clustering against experimental gas-detector measurements [6, 7].

Within the framework of the six-week INTEREST Wave 14 internship at LRB JINR, this study was conducted to bridge the gap between physical validation and biological application. The internship focused on three primary objectives:

1. **Macroscopic Physical Validation:** To systematically validate the Geant4-DNA and EM Standard physics lists by evaluating continuous transport parameters — namely stopping power, CSDA range, and detour factor — for protons, alpha particles, and ^{12}C ions against the recognized standard data

from ICRU Report 90.

2. **Microscopic (Nanodosimetric) Validation:** To evaluate the accuracy of Geant4-DNA models in simulating the Ionisation Cluster Size Distribution (ICSD). This was achieved by accurately replicating the geometric and thermodynamic conditions of the StarTrack and PTB experimental nanodosimetry setups for a wide range of light and heavy ions.

3. **Modeling of Sub-cellular Biostructures:** To apply the validated physics models to estimate the ICSD within the effective volumes of critical sub-cellular structures (Histones, Ribosomes, Cytoskeleton segments, and NMDA receptors). By simulating irradiation with GCR-relevant ions (protons, deuterons, alpha particles, ^{6}Li, ^{7}Li, ^{12}C, and ^{20}Ne) at 1 MeV/u in high-density biological environments, this task provides a quantitative foundation for evaluating localized macromolecular radiation damage.

I ICRU90 validation

Problem Statement

Before investigating the nanometric pattern of energy deposition (such as ionisation clustering) induced by ionizing radiation, it is absolutely essential to ensure that the macroscopic transport parameters of the primary particles are simulated accurately. The macroscopic behavior of a particle traversing a medium is governed by continuous energy loss and multiple scattering, which dictate its penetration depth and the amount of energy deposited per unit path length.

If a Monte Carlo simulation fails to correctly reproduce basic macroscopic observables—such as the rate of energy loss or the total range of a particle—any subsequent nanodosimetric calculations or biological damage estimations will be inherently flawed. Therefore, the primary problem addressed in this section is the systematic validation of the Geant4-DNA physical models against internationally recognized standard reference data. By comparing the simulated macroscopic quantities against the gold-standard data, we can identify the limits of applicability (especially at low energies) for each Geant4 electromagnetic physics constructor.

Physics Lists in Geant4

Geant4 provides the capability to simulate various processes, including particle transport, electromagnetic and hadronic interactions, decay, and optical phenomena. For any given task, a specific set of particles and processes, described by a collection of models, must be selected. Such a combination is referred to as a *physics list*.

In the context of this study, the focus is on electromagnetic (EM) physics lists, as they enable the modeling of ionization processes, which are the primary source of delta-electrons.

Among the available electromagnetic physics lists, the following five are investigated in this work: EM Standard Option 4 and DNA Options 2, 4, 6, and 8. This selection is based on the following reasons:

1. To confirm the necessity of developing dedicated DNA physics lists: standard physics lists (e.g., EM Standard Option 4) are currently not adapted to model ionization losses at extremely low energies and small spatial scales event-by-event.

2. To evaluate and compare the simulation quality offered by different DNA physics lists across different ions and energy regimes.

The distinction between the proposed physics lists lies not only in the different models and applicable particles but also in the fundamental approach upon which the EM Standard and DNA lists are based. EM Standard physics lists are developed based on the *Condensed History* approach, which groups many small energy-loss collisions into single macroscopic steps. Conversely, DNA physics lists rely on the *Detailed Track Structure* approach, simulating every single interaction (ionization, excitation, elastic scattering) down to the electron-volt scale.

Let us examine the content of these physics lists in greater detail. The models used in EM Standard physics lists are presented in Table 1. The corresponding models used in DNA physics lists (Options 2, 4, 6, and 8) incorporate specific analytical and semi-empirical cross-sections tailored for liquid water.

Table 1 – Summary of electromagnetic models utilized in the EM Standard Option 4 physics list for ion transport.

Model	**Applicability (Particle & Energy)**	**Based on Data / Theory**
G4BetheBlochModel	Default high-energy model for protons and heavy ions (> 2 MeV/u)	Bethe-Bloch theory with Barkas and Bloch corrections
G4LindhardSorensenModel	Heavy ions ($Z > 2$) at high energies	ICRU73 & ICRU90
G4BraggModel	Protons (< 2 MeV) and backup for all ions (incorporates effective charge)	ICRU90 & PSTAR
G4BraggIonModel	Alpha particles (< 2 MeV/u)	ICRU90 & ASTAR

ICRU90 Reference Data and Physical Quantities

ICRU Report 90 [8] (Key Data for Ionizing-Radiation Dosimetry) provides the internationally recognized quantitative standard for the transport of protons, alpha particles, ^{12}C ions, electrons, and positrons in key materials: air, graphite, and liquid water.

Because Geant4-DNA is explicitly developed for radiobiology, liquid water is used as the primary surrogate for biological tissue. Therefore, all validations in this section are performed exclusively in liquid water.[1]

To comprehensively validate the macroscopic transport of ions in Geant4, three fundamental physical quantities defined by ICRU90 were extracted and compared:

1. **Electronic Stopping Power (S_{el}/ρ):** The mean energy lost by a charged particle per unit path length due to inelastic collisions (ionizations and excitations) with atomic electrons, divided by the density of the medium. It is expressed as:

$$\frac{S_{el}}{\rho} = \frac{1}{\rho}\left(\frac{dE}{dl}\right)_{el} \tag{1}$$

2. **CSDA Range (R_{csda}):** The Continuous-Slowing-Down Approximation range is the theoretical path length a particle would travel if it continuously lost energy at a rate given by the stopping power. It is calculated by integrating the reciprocal of the total stopping power from the initial energy T_0 down to zero:

$$R_{csda} = \int_0^{T_0} \frac{1}{S(T)} dT \tag{2}$$

[1] While the current focus is on liquid water, it is expected that future developments in Geant4-DNA will include cross-sections for other biological molecules such as DNA backbones or proteins.

3. **Detour Factor (D):** The ratio of the mean projected penetration depth (along the initial direction of motion) to the CSDA range. Since particles undergo multiple elastic scattering (which deflects their trajectory), the actual penetration depth is less than the total path length. A detour factor close to 1 implies straight-line transport, while a drop in the detour factor highlights the increasing importance of elastic scattering at low energies.

Results

In the following figures, the simulated data from Geant4 EM Standard Option 4 and DNA Options (2, 4, 6, and 8) are compared against the ICRU90 reference data. **Note on graphical representation:** If only one DNA option (e.g., DNA Opt2) is depicted in a plot, it signifies that the curves for the other DNA options (Opt4, Opt6, Opt8) perfectly coincide with it. If multiple DNA options are explicitly shown, it indicates a measurable divergence between the track structure models. The bottom panels of all graphs show the relative residual error $\eta = 1 - \text{Geant4/Exp}$.

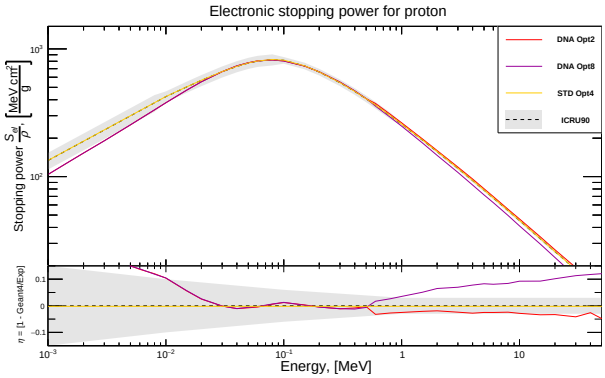

(a) Electronic Stopping power for proton

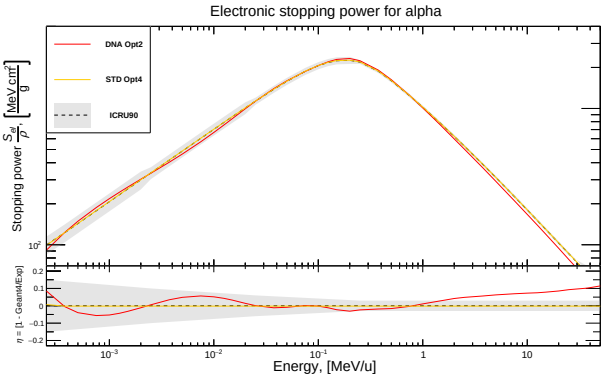

(b) Electronic Stopping power for alpha

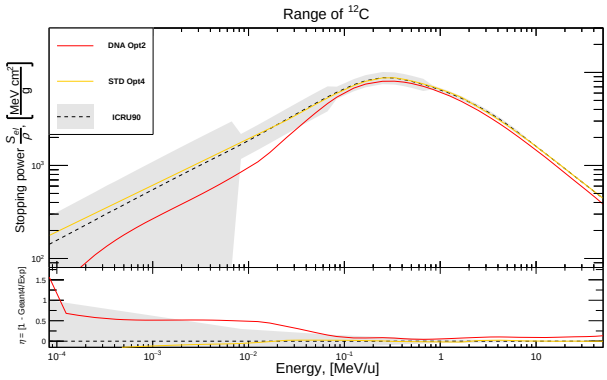

(c) Electronic Stopping power for ^{12}C

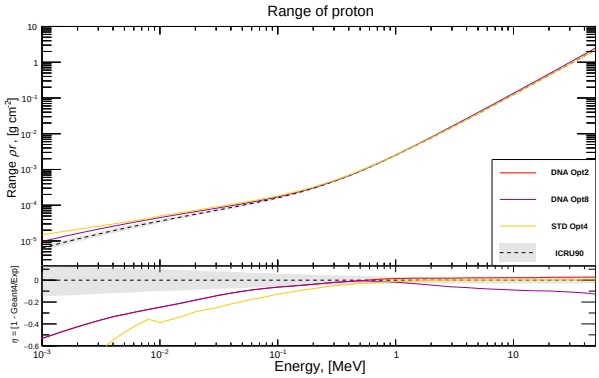

(a) Range for proton

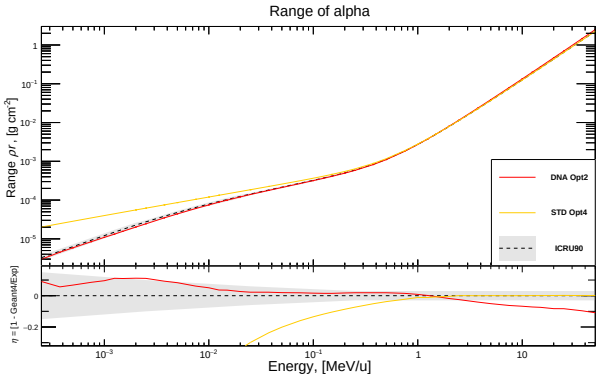

(b) Range for alpha

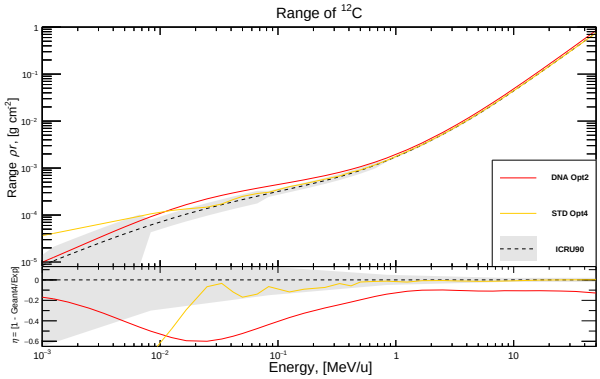

(c) Range for ^{12}C

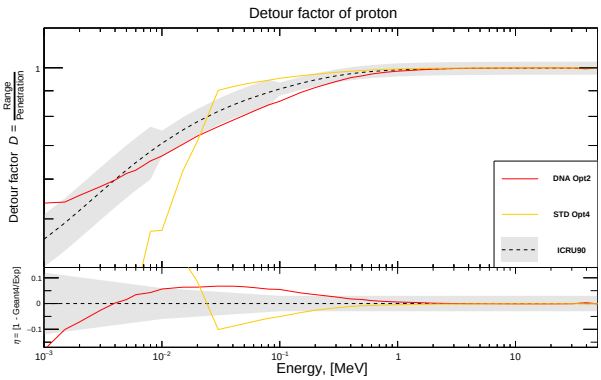

(a) Detour factor for proton

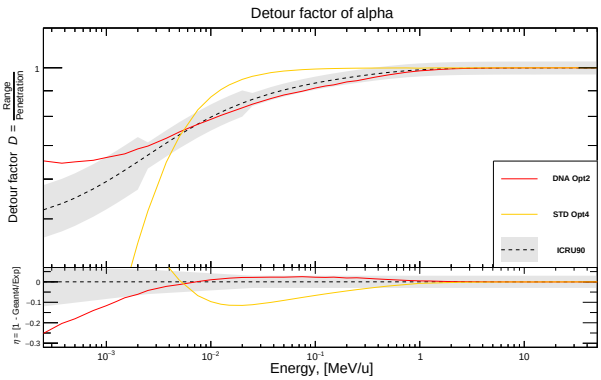

(b) Detour factor for alpha

Analysis of Macroscopic Validation

The validation results highlight a fundamental difference between the Condensed History (Standard) and Track Structure (DNA) approaches. **STD Option 4** directly utilizes parameterized tables from ICRU databases (as outlined in Table 1). Consequently, for almost all ions and quantities, STD Opt4 perfectly aligns with the ICRU90 reference curve (the residual $\eta \approx 0$). Conversely, **Geant4-DNA options** compute energy loss dynamically based on individual interaction cross-sections (first-principles approach). Comparing DNA options to ICRU90 tests the macroscopic accuracy of these microscopic cross-sections.

- **Protons:** For the electronic stopping power (Fig. 1a), DNA options generally show good agreement above 10^{-2} MeV. However, DNA Opt8 shows a slight systematic underestimation at higher energies

compared to Opt2/Opt4. The range (Fig. 2a) is accurately reproduced by all models. The detour factor (Fig. 3a) reveals that while STD Opt4 accurately handles multiple scattering down to low energies, the DNA models begin to underestimate the detour factor below 10^{-2} MeV, indicating overly aggressive elastic scattering cross-sections at the extreme low-energy limit.

- **Alpha particles:** Stopping power and range (Fig. 1b, 2b) are highly accurate for DNA options down to 10^{-1} MeV/u. Below this threshold, the DNA models overestimate the stopping power by up to 10%, resulting in a slight underestimation of the range. The detour factor (Fig. 3b) follows the same trend as protons, where DNA options struggle at extremely low energies ($< 10^{-2}$ MeV/u).

- **Carbon (^{12}C):** The stopping power for carbon (Fig. 1c) reveals significant limitations in the current DNA cross-sections for heavy ions. Below 10^{-1} MeV/u, the DNA options severely underestimate the stopping power (residual reaching -0.6). Consequently, because the simulated carbon ion loses energy too slowly, its simulated range (Fig. 2c) is severely overestimated at low energies. STD Opt4, relying on empirical tables, avoids this issue entirely.

A summary of the physics lists performance regarding macroscopic validation is provided in Table 2.

Table 2 – Summary of physics lists performance regarding ICRU90 macroscopic validation. (DNA options behave similarly to each other for alpha and carbon; Opt2 is listed as the representative default).

Ion	Physical Quantity	Best Performing List	Major Discrepancies
Proton	Stopping Power	STD Opt4, DNA Opt2/4/6	DNA Opt8 (slight deviation at high E)
	Range	All models perform well	–
	Detour Factor	STD Opt4	DNA Options (underestimate at $< 10^{-2}$ MeV)
Alpha	Stopping Power	STD Opt4	DNA Options (overestimate at $< 10^{-2}$ MeV/u)
	Range	STD Opt4	DNA Options (slight underestimate at low E)
	Detour Factor	STD Opt4	DNA Options (underestimate at $< 10^{-2}$ MeV/u)
^{12}**C**	Stopping Power	STD Opt4	DNA Options (severe underestimate at $< 10^{-1}$ MeV/u)
	Range	STD Opt4	DNA Options (severe overestimate at $< 10^{-1}$ MeV/u)

Conclusion: For macroscopic transport (dose deposition depth, total range), **STD Option 4** remains the most reliable choice across all energy ranges due to its direct reliance on ICRU data. However, **Geant4-DNA** models maintain an acceptable macroscopic accuracy for protons and alphas at therapeutic energies (> 1 MeV/u), which justifies their use for nanodosimetry. Caution must be applied when using current DNA physics lists for heavy ions like ^{12}C at very low energies (the Bragg peak Bragg/fragmentation tail), as the underlying cross-sections currently lead to measurable macroscopic transport errors.

II Validation by Experimental data

Problem statement

The accurate assessment of radiation-induced biological damage, particularly in the context of hadron therapy and space radiobiology, requires a transition from the macroscopic concept of absorbed dose to the microscopic characterization of particle tracks. While the absorbed dose quantifies the mean energy imparted to a macroscopic mass, it fails to capture the highly stochastic nature of energy deposition events at the scale of sub-cellular structures, such as the DNA molecule (approximately 2 nm in diameter) or nucleosomes (around 10 nm).

The key to understanding the relative biological effectiveness (RBE) of light and heavy ions lies in their track structure—the spatial distribution of inelastic interactions (ionisations and excitations) produced by the primary particle and its secondary electrons (δ-rays). Since biological responses, such as clustered double-strand breaks (DSBs), are triggered by multiple ionisation events occurring in close spatial proximity, validating Monte Carlo codes like Geant4-DNA at the nanometric scale is of utmost importance.

The problem addressed in this section is the systematic validation of various Geant4-DNA electromagnetic physics constructors (specifically DNA Option 2, Option 4, Option 6, and Option 8) against experimental nanodosimetry data. Since direct measurement of ionisation clusters in liquid water at the nanometer scale is currently technologically impossible, experimental data are obtained using macroscopic volumes of low-pressure tissue-equivalent gases (such as propane) which simulate nanometric volumes of liquid water. Therefore, the Geant4-DNA simulations must accurately replicate not only the physical interactions but also the specific geometric and thermodynamic conditions of the experimental setups.

Experimental Setups and Geometries

To perform a comprehensive validation, the Geant4-DNA simulations were tailored to replicate two distinct experimental nanodosimetry setups. These setups utilize low-pressure propane (C_3H_8) to simulate nanometer-sized volumes of liquid water, relying on the scaling of the mean free path of ionisation.

1. StarTrack Setup [6]

The StarTrack apparatus, installed at the Legnaro National Laboratories of INFN (LNL-INFN), is based on a single-electron counting technique. The detector features an almost wall-less cylindrical target volume. In the experimental conditions, the chamber is filled with propane gas at a pressure of 3 mbar. At this specific pressure, the physical dimensions of the cylindrical target volume (3.7 mm in diameter and height) correspond to a mass thickness of about 2 $\mu g/cm^2$. Applying the density scaling to liquid water (density 1 g/cm^3), this macroscopic gas volume effectively simulates a nanometric cylinder of liquid water exactly **20 nm in diameter and 20 nm in height**. This dimension is comparable to the size of a chromatin

fiber. The StarTrack setup measures the ionisation cluster size by extracting and amplifying the secondary electrons produced by a passing primary ion using a multi-step avalanche chamber (MSAC). This geometry was explicitly modeled in Geant4 to validate the tracks of Protons, Deuterons, and Lithium ions.

2. PTB Nanodosimeter Setup [7]

The nanodosimeter developed at the Physikalisch-Technische Bundesanstalt (PTB) operates on a different principle: positive ion counting. The interaction region is located between the electrodes of a parallel plate capacitor filled with propane gas at a lower pressure of 1.2 mbar. Instead of extracting electrons, this setup extracts the positive ions created in the target gas towards a secondary electron multiplier. At 1.2 mbar, utilizing the appropriate scaling factors for the ionisation cross-sections of propane relative to water, the effective size of the target volume is equivalent to a liquid water cylinder with a diameter of $D \approx 2.3$ nm and a height of $H \approx 6.1$ nm. This extremely small volume perfectly matches the dimensions of a **short DNA segment** (approximately two turns of the DNA double helix). The PTB geometry was modeled in Geant4 to validate the highly dense tracks of 1 MeV/u Alpha particles and 7.33 MeV/u ^{12}C ions.

Ionisation cluster size distribution (ICSD)

The Ionisation Cluster Size Distribution (ICSD) is the fundamental observable in experimental nanodosimetry and a critical metric for evaluating radiation quality. Mathematically, the ICSD is represented as a discrete probability distribution, $P_\nu(Q, d)$, which defines the probability that exactly ν ionisation events are created within a specified target volume V by a single primary particle of radiation quality Q (defined by its mass, charge, and velocity) passing at an impact parameter d from the center of the volume.

By definition, the sum of all probabilities must equal unity:

$$\sum_{\nu=0}^{\infty} P_\nu(Q, d) = 1 \tag{3}$$

The cluster size ν acts as a surrogate for the complexity of initial DNA damage. For instance, an event with $\nu = 1$ or $\nu = 2$ might correspond to simple, easily repairable single-strand breaks (SSBs). However, events with $\nu \geq 3$ within a 2 nm target are strongly correlated with the induction of clustered DNA lesions and lethal double-strand breaks (DSBs), which are notoriously difficult for cellular repair mechanisms to process correctly.

The shape of the ICSD depends heavily on the particle's track structure. It comprises two main components:

- **Track-core region:** When the primary ion directly traverses the target volume (small impact parameter d), the ICSD is dominated by the primary particle's direct ionisations. The distribution typically exhibits a peak at a higher ν value, which is inversely proportional to the mean free path of ionisation (λ_{ion}) of the particle.

- **Penumbra region:** When the primary ion passes outside the target volume, the ionisations inside the volume are caused exclusively by secondary electrons (δ-rays). In this case, the probability P_0 (zero ionisations) is overwhelmingly large, and the distribution for $\nu \geq 1$ drops exponentially.

By comparing the experimental ICSD with the ICSD obtained from Geant4-DNA simulations, we can rigorously test the accuracy of the underlying electromagnetic cross-sections (ionisation, excitation, elastic scattering) implemented in the different physics options (Opt2, Opt4, Opt6, Opt8).

Results

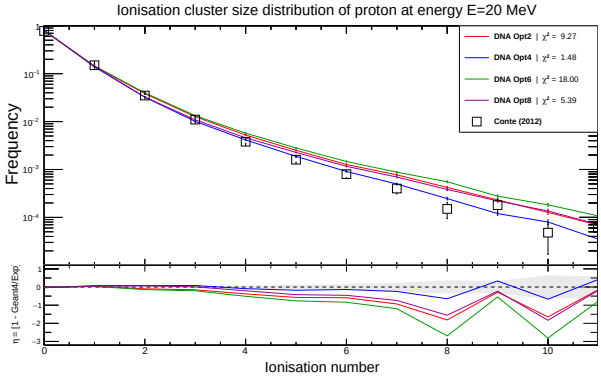

(a) ICSD of proton at energy $E = 20$ MeV

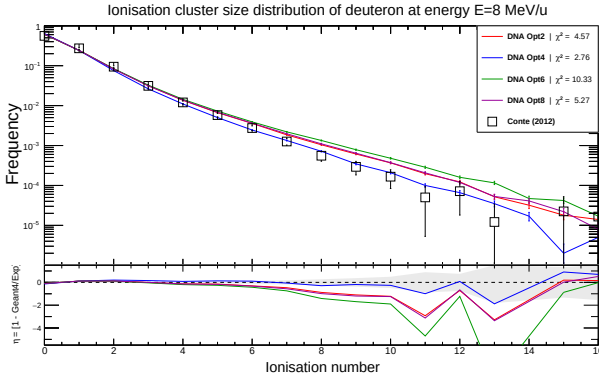

(b) ICSD of deuteron at energy $E = 8$ MeV/u

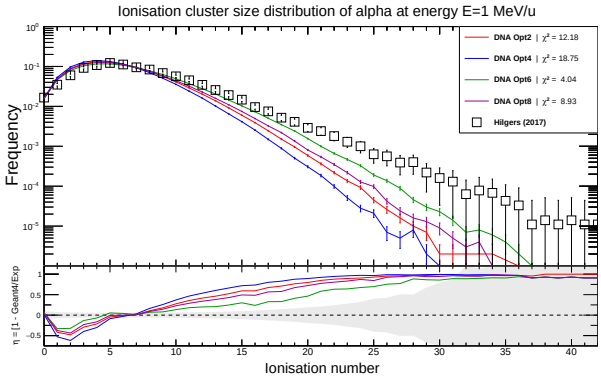

(c) ICSD of alpha at energy $E = 1$ MeV/u

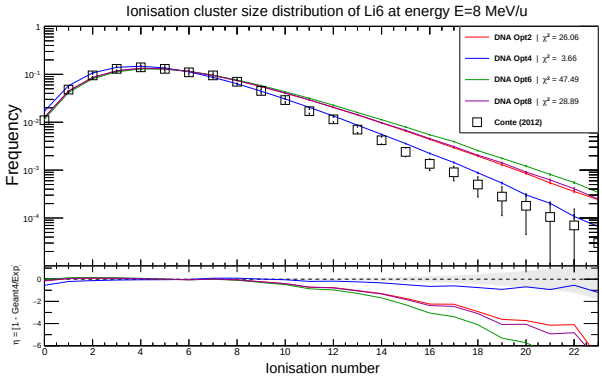

(d) ICSD of ^{7}Li at energy $E = 8$ MeV/u

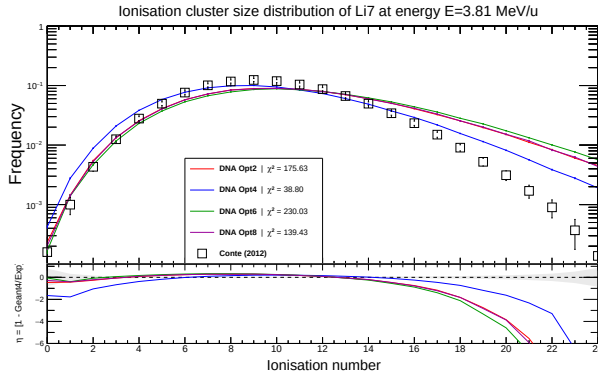

(e) ICSD of ^{7}Li at energy $E = 3.81$ MeV/u

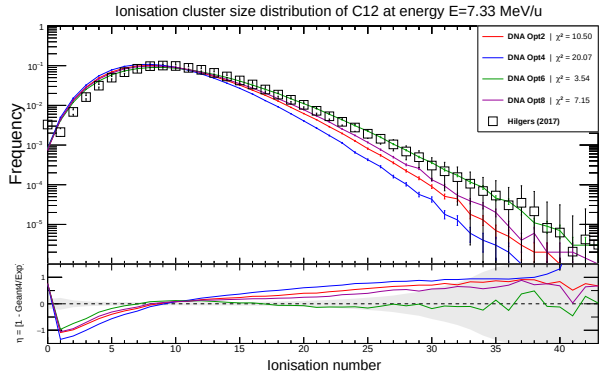

(f) ICSD of ^{12}C at energy $E = 7.33$ MeV/u

The simulated ICSDs for various ions were compared against experimental data from Conte et al. [6] and Hilgers et al. [7].. To quantitatively evaluate the agreement between the Geant4-DNA simulations and the experimental data, a χ^2 goodness-of-fit test was performed for each physics constructor (DNA Opt2, Opt4, Opt6, and Opt8). The bottom panels of the graphs display the residual parameter $\eta = 1 - \text{Geant4/Exp}$, which visually highlights the relative deviation of the Monte Carlo results from the experimental points.

A summary of the statistical evaluation is presented in Table 3, identifying the best and worst performing physics options for each ion configuration.

Table 3 – Summary of χ^2 evaluations for ICSD simulations across different ions and experimental setups. The best and worst performing Geant4-DNA physics options are highlighted.

Primary Ion	**Energy**	**Exp. Setup (Volume)**	**Best Option (χ^2)**	**Worst Option (χ^2)**
Proton (^{1}H)	20 MeV	StarTrack (20 nm)	**Opt4** (1.48)	Opt6 (18.00)
Deuteron (^{2}H)	8 MeV/u	StarTrack (20 nm)	**Opt4** (2.76)	Opt6 (10.33)
Alpha (^{4}He)	1 MeV/u	PTB (2.3 nm)	**Opt6** (4.04)	Opt4 (18.75)
Lithium (^{6}Li)	8 MeV/u	StarTrack (20 nm)	**Opt4** (3.66)	Opt6 (47.49)
Lithium (^{7}Li)	3.81 MeV/u	StarTrack (20 nm)	**Opt4** (38.80)	Opt6 (230.03)
Carbon (^{12}C)	7.33 MeV/u	PTB (2.3 nm)	**Opt6** (3.54)	Opt4 (20.07)

Analysis of Results by Ion and Geometry

1. Light Ions in 20 nm volumes (Proton, Deuteron, Lithium): Figures 4a, 4b, 4f, and 4e depict the ICSD for H, D, and Li isotopes simulated inside the 20 nm StarTrack geometry. For all these ions, **DNA Option 4** demonstrates superior performance. As seen in the proton distribution (Fig. 4a), Opt4 ($\chi^2 = 1.48$) perfectly traces the experimental tail for higher cluster sizes, whereas Opt6 consistently underestimates the probability of zero-ionisation and small clusters while overestimating large cluster sizes (yielding the worst $\chi^2 = 18.00$). This trend is strongly preserved for Deuterons (Fig. 4b) and ^{6}Li (Fig. 4f).

In the case of the slower, more densely ionizing ^{7}Li at 3.81 MeV/u (Fig. 4e), the distribution shifts to form a distinct peak around $\nu = 9$. While all models struggle slightly to capture the exact height of the experimental peak (resulting in globally higher χ^2 values), Option 4 still provides the most accurate estimation ($\chi^2 = 38.80$), whereas Option 6 severely overestimates the large cluster tail, dropping to a χ^2 of 230.03. This suggests that for relatively larger nanometric volumes (20 nm) and standard light ions, the cross-sections utilized in DNA Option 4 (which represent the most detailed standard electromagnetic models in Geant4) provide the most accurate spatial distribution of delta-ray ranges and ionisation clustering.

2. Heavy/Slow Ions in 2 nm volumes (Alpha, Carbon): A distinct paradigm shift is observed in Figures 4c and the final subfigure for ^{12}C. These simulations replicate the PTB setup, representing an ultra-small 2.3 nm volume subjected to high-LET particles. Here, **DNA Option 6** significantly outperforms all other lists. For the 1 MeV/u Alpha particle, Opt6 perfectly matches the broad distribution extending up to 40 ionisations ($\chi^2 = 4.04$). Conversely, Option 4 severely underestimates the probability of large clusters (falling into the $\eta = -0.5$ residual region), yielding a poor χ^2 of 18.75.

Similarly, for the ^{12}C ion at 7.33 MeV/u, Option 6 ($\chi^2 = 3.54$) elegantly tracks the plateau and subsequent drop-off of the experimental data up to $\nu = 45$. Option 4 ($\chi^2 = 20.07$) again drops too early,

underestimating the dense clustering effect of the carbon track core.

Conclusion on Physics Lists: The results clearly indicate a geometry- and LET-dependent suitability of the Geant4-DNA physics constructors. **DNA Option 4** is highly recommended for standard proton/light-ion therapy simulations where target volumes are in the range of nucleosomes or chromatin fibers (∼10–20 nm). However, for high-LET particles (like low-energy alphas and carbon ions) evaluated at the direct DNA scale (∼2 nm), **DNA Option 6** is strictly necessary. Option 6 includes specifically tailored cross-sections (such as the CPA100 models) that better handle the intense, highly localized dense ionisation clouds characteristic of the track core of heavy ions, preventing the underestimation of clustered damage that occurs with Option 4.

III Simulation of ICSD on biostructures

Problem Statement

While the validation of Geant4-DNA physics lists against experimental nanodosimetry data provides confidence in the accuracy of the track structure models, the ultimate goal of computational radiobiology is to assess radiation damage within actual biological targets.

In typical Monte Carlo simulations, biological cells are often approximated as homogeneous volumes of liquid water at a standard density of 1.0 g/cm^3. However, real sub-cellular structures—such as proteins, nucleic acids, and lipid membranes—are highly compacted and possess a significantly higher physical density than bulk water. To more accurately estimate the localized energy deposition and the resulting Ionisation Cluster Size Distribution (ICSD) inside these critical targets, it is necessary to adjust the physical density of the medium to reflect the highly packed nature of biological macromolecules.

In this study, the biological structures are modeled using water as the base material, but its density is artificially increased to 1.407 g/cm^3. This value effectively accounts for the average mass density of typical dry proteins and dense biological complexes. The objective of this section is to simulate the ICSD produced by various ions (protons, deuterons, α, ^{6}Li, ^{7}Li, ^{12}C, and ^{20}Ne) at a specific therapeutic energy of 1 MeV/u directly within the effective volumes of key sub-cellular structures. This approach allows us to quantify the complexity of the damage induced by high-LET (Linear Energy Transfer) particles at the fundamental biological level.

Sub-cellular structures

To evaluate the ICSD, four distinct sub-cellular structures were selected based on their critical roles in cellular function and survival. To optimize computational efficiency while preserving the accurate mass-thickness and geometric cross-section of the targets, these complex biological macromolecules were approximated using standard Geant4 geometric primitives (such as solid cylinders, hollow tubes, and spheres). Complex CAD-based geometries require significantly more computational overhead for boundary crossing calculations, whereas simple primitives capture the exact stochastics of energy deposition required for ICSD analysis.

The four structures investigated are:

- **Cytoskeleton (Microtubule segment):** The cytoskeleton provides structural support to the cell and is essential for intracellular transport and cell division. Microtubules are hollow cylindrical structures. In our model, a short segment of a microtubule is represented as a hollow tube.
- **NMDA receptor:** The N-methyl-D-aspartate (NMDA) receptor is a crucial transmembrane ion channel protein found in nerve cells, vital for synaptic plasticity and memory function. It is modeled as an elongated solid cylinder traversing the cell membrane.

- **Histone:** Histones are highly alkaline proteins found in eukaryotic cell nuclei that package and order the DNA into structural units called nucleosomes. Due to its compact, globular nature, the histone core is modeled as a small solid primitive.

- **Ribosome:** Ribosomes are large, dense macromolecular complexes responsible for protein synthesis (translation). Due to its substantial size compared to other selected proteins, it is modeled as a large solid primitive.

The geometric parameters applied in the Geant4 application to construct these biological targets are summarized in Table 4.

Table 4 – Geometric parameters and density configurations used for modeling the selected sub-cellular structures in Geant4-DNA.

Structure	**Geom. Primitive**	**Inner Radius**	**Outer Radius**	**Height**	**Density**
Cytoskeleton	Hollow Tube	7.5 nm	12.5 nm	8.0 nm	1.407 g/cm^3
NMDA receptor	Solid Cylinder	0.0 nm	4.0 nm	18.0 nm	1.407 g/cm^3
Histone	Solid Sphere	0.0 nm	2.5 nm	–	1.407 g/cm^3
Ribosome	Solid Sphere	0.0 nm	12.5 nm	–	1.407 g/cm^3

Results

The simulated Ionisation Cluster Size Distributions (ICSD) for the aforementioned sub-cellular structures irradiated by various ions at an energy of 1 MeV/u are presented below.

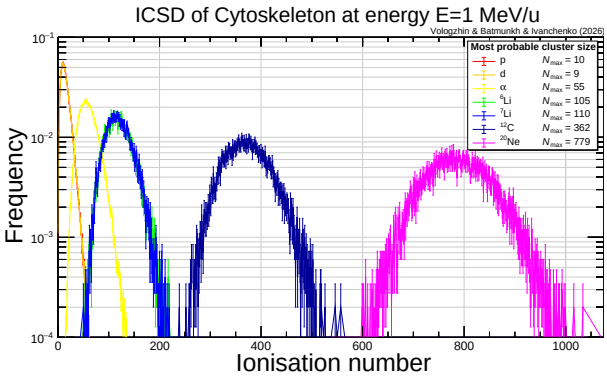

(a) ICSD of Cytoskeleton at energy $E = 1$ MeV/u

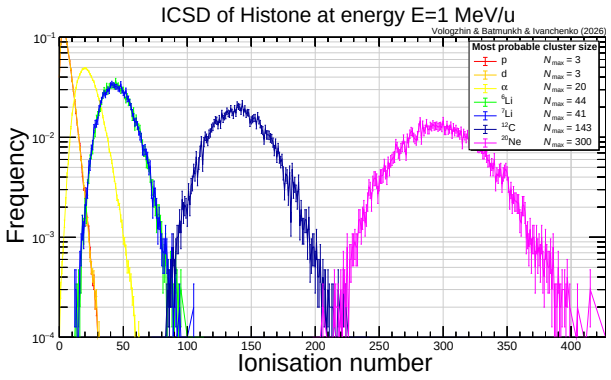

(b) ICSD of Histone at energy $E = 1$ MeV/u

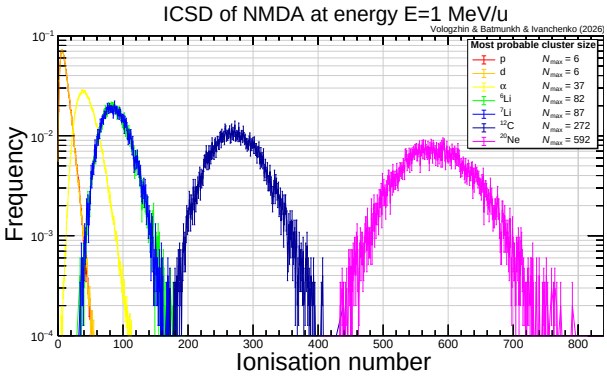

(c) ICSD of NMDA receptor at energy $E = 1$ MeV/u

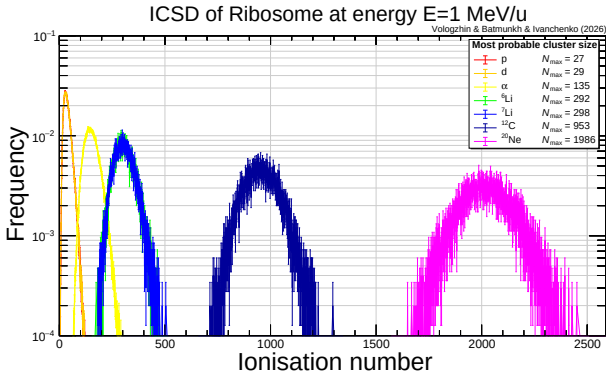

(d) ICSD of Ribosome at energy $E = 1$ MeV/u

Analysis of Biological ICSD

The simulated distributions clearly demonstrate the dramatic impact that both the particle's atomic number (Z) and the target's physical dimensions have on the degree of ionisation clustering. The *most probable cluster size* (N_{max}) serves as an excellent indicator of the localized damage severity.

- **Impact of Particle Type (LET effect):** Across all four targets, keeping the specific energy constant at 1 MeV/u, an increase in the mass and charge of the primary ion leads to an extreme shift of the ICSD towards higher values. For instance, in the Cytoskeleton (Fig. 5a), the most probable cluster size is $N_{max} = 10$ for protons, but it increases drastically to $N_{max} = 362$ for ^{12}C, and reaches an enormous $N_{max} = 779$ for ^{20}Ne. This vividly illustrates the concept of Relative Biological Effectiveness (RBE) of heavy ions: a single ^{20}Ne ion traversing a microtubule segment completely shatters the molecular structure by inducing nearly 800 ionisations in a nanometric space, almost guaranteeing irreversible denaturation of the protein.

- **Impact of Target Volume:** By comparing the different biological structures, we observe the volume-dependence of the ICSD. The Histone (Fig. 5b), being the smallest structure ($R_{out} = 2.5$ nm), exhibits the lowest cluster sizes overall, with $N_{max} = 3$ for protons and $N_{max} = 300$ for ^{20}Ne. Conversely, the Ribosome (Fig. 5d) represents the largest target mass. Consequently, it absorbs significantly more energy from the track core, leading to $N_{max} = 27$ for protons and an astonishing $N_{max} = 1986$ for ^{20}Ne.

- **Isotope comparison:** Interestingly, comparing the two Lithium isotopes (^{6}Li and ^{7}Li) at the same specific energy (1 MeV/u) shows that their macroscopic track structures and resulting cluster sizes are remarkably similar. For the NMDA receptor (Fig. 5c), $N_{max} = 82$ for ^{6}Li and $N_{max} = 87$ for ^{7}Li. The minor differences are primarily attributed to the slightly different velocities and corresponding delta-ray spectra.

Future Outlook: Implementing BEB Cross-Sections

While scaling the density of liquid water to 1.407 g/cm^3 provides a realistic approximation of the mass-stopping power within biological targets, it is still a simplification. Biological macromolecules are composed of Carbon, Nitrogen, Oxygen, Phosphorus, and Sulfur, which have different electronic shell structures and ionisation potentials compared to the H_2O molecule.

The results obtained in this section establish a highly robust baseline. Future research within the framework of this project will focus on evaluating how these baseline ICSD values change when the explicit ionisation cross-sections of actual biomolecules are used instead of scaled water. Such molecular-specific cross-sections can be analytically calculated using the Binary Encounter Bethe (BEB) model. Comparing the current high-density water approximations against future BEB-derived biological cross-sections will definitively reveal the necessity (or lack thereof) of implementing molecule-specific material tracking in Geant4-DNA for advanced radiobiology.

Conclusion

Over the course of the six-week INTEREST Wave 14 internship at the Laboratory of Radiation Biology (LRB JINR), a comprehensive computational study focusing on the track structure and nanodosimetry of ionizing radiation was successfully conducted using the Geant4-DNA toolkit (version 11.4 ref02). The following key results were obtained:

1. **Macroscopic Validation (ICRU90):** Macroscopic transport parameters, including electronic stopping power, CSDA range, and detour factor, were validated against ICRU90 reference data for protons, alpha particles, and ^{12}C ions in liquid water. It was established that while the EM Standard Option 4 perfectly reproduces the empirical ICRU90 data, the Geant4-DNA physics lists exhibit measurable deviations at extremely low energies (e.g., below 10^{-1} MeV/u for carbon). This highlights current limitations in microscopic cross-sections for heavy ions at the very end of their particle tracks.

2. **Microscopic Validation (ICSD):** The Ionisation Cluster Size Distribution (ICSD) was rigorously vvalidated against experimental nanodosimetry data from the StarTrack [6] and PTB [7] setups. The evaluated models included EM Standard Option 4 and DNA Options 2, 4, 6, and 8 for a wide range of ions (protons, deuterons, α, ^{6}Li, ^{7}Li, and ^{12}C). As expected, the Condensed History approach (EM Standard) proved entirely unsuitable for estimating discrete ionizations at the DNA scale.

3. **Physics Lists Assessment:** It was determined that the optimal Geant4-DNA physics list is highly dependent on both the target volume size and the particle's Linear Energy Transfer (LET). **DNA Option 4** is the most accurate for light ions in larger nanometric volumes ($\sim$20 nm). However, **DNA Option 6** is strictly necessary to accurately capture the dense ionization clustering of high-LET particles (such as low-energy alphas and ^{12}C) at the fundamental DNA scale ($\sim$2.3 nm), primarily due to its advanced electron transport modeling based on CPA100 cross-sections.

4. **Sub-cellular Biostructure Modeling:** The ICSD was successfully simulated directly within approximated geometric models of critical biological structures (Cytoskeleton, NMDA receptor, Histone, and Ribosome). By utilizing a biologically relevant high-density water approximation (1.407 g/cm^3), the study clearly demonstrated the extreme LET- and volume-dependence of ionization clustering. This provides a robust physical baseline for estimating the complexity of radiation-induced macromolecular damage.

The results obtained establish a solid foundation for future research. Specifically, the high-density water baseline generated for biostructures will be used to evaluate the impact of implementing explicit, molecule-specific ionization cross-sections calculated via the Binary Encounter Bethe (BEB) procedure.

These findings will be incorporated into a forthcoming validation article planned for submission to *Medical Physics*, combining the outcomes of both the current INTEREST internship and the preceding START internship program.

We emphasize the strategic importance of this internship, as it fostered productive collaboration between researchers at the Laboratory of Radiation Biology (LRB JINR) and the Laboratory of High Energy Physics Data Analysis (LHEPDA TSU) aimed at studying the complex effects of cosmic and therapeutic radiation on biological structures.

The intern plans to actively continue this research and collaboration with the scientific supervisor within the ongoing framework of the INTEREST program.

References

1. Batmunkh M., Bayarchimeg L., Bugay A.N. Mathematical modeling of radiation-induced effects in structures of the central nervous system under the action of heavy charged particles. — Dubna: Joint Institute for Nuclear Research, 2024. — (JINR Preprint P11-2024-49).

2. Batmunkh M., Bayarchimeg L., Bugay A.N., Lkhagva O. Computer simulation of radiation damage mechanisms in the structure of brain cells // Proceedings of the 24th International Scientific Conference of Young Scientists and Specialists (AYSS-2020). — Dubna, 2021. — P. 050001. — DOI: 10.1063/5.0063370.

3. Bulanova T.S., Boreyko A.V., Zadneprianetc M.G., Krasavin E.A., Kulikova E.A. Formation of DNA Double-Strand Breaks in Rat Brain Neurons after Irradiation with Krypton Ions (^{78}Kr) // Physics of Particles and Nuclei Letters. — 2019. — Vol. 16, No. 4. — P. 402–408. — DOI: 10.1134/s1547477119040083.

4. Nikjoo H., Uehara S., Wilson W.E., Hoshi M., Goodhead D.T. Track structure in radiation biology: theory and applications // International Journal of Radiation Biology. — 1998. — Vol. 73, No. 4. — P. 355–364.

5. Vasil'eva M., Dushanov E., Bugay A. Modeling of DNA damage repair induced by heavy ions in mammalian cells // Russian Journal of Biological Physics and Chemistry. — 2022. — Vol. 7, No. 4. — P. 557–564. — DOI: 10.29039/rusjbpc.2022.0560.

6. Conte V., Colautti P., Grosswendt B. et al. Track structure of light ions: experiments and simulations // New Journal of Physics. — 2012. — Vol. 14. — P. 093010. — DOI: 10.1088/1367-2630/14/9/093010.

7. Hilgers G., Bug M.U., Rabus H. Measurement of track structure parameters of low and medium energy helium and carbon ions in nanometric volumes // Physics in Medicine & Biology. — 2017. — Vol. 62. — P. 7569–7597. — DOI: 10.1088/1361-6560/aa86e8.

8. ICRU. Key Data for Ionizing-Radiation Dosimetry: Measurement Standards and Applications. ICRU Report 90 // Journal of the ICRU. — 2014. — Vol. 14, No. 1. — Oxford University Press. — DOI: 10.1093/jicru/ndw032.

9. Incerti S., Kyriakou I., Bernal M. A. et al. Geant4-DNA example applications for track structure simulations in liquid water: a report from the Geant4-DNA Project // Medical Physics. — 2018. — Vol. 45, No. 8. — P. e722-e739. — DOI: 10.1002/mp.13048.